Castrejon-Pita, J.R., Castrejon-Pita, A.A., Hinch, E.J., Lister, J.R., Hutchings, I.M., Physical Review (in press 2012) 'Self-similar Breakup of Near-inviscid Fluids'

Self-similar Breakup of Near-inviscid Fluids

J.R. Castrejón-Pita, A.A. Castrejón-Pita, E.J. Hinch[♮], J.R. Lister[♮], and I.M. Hutchings
Department of Engineering, University of Cambridge,
17 Charles Babbage Road, Cambridge, CB3 0FS, U.K. and
[♮]*Department of Applied Mathematics and Theoretical Physics,*
University of Cambridge, Cambridge, CB3 9EW, U.K.

The final stages of pinchoff and breakup of dripping droplets of near-inviscid Newtonian fluids are studied experimentally for pure water and ethanol. High speed imaging and image analysis are used to determine the angle and the minimum neck size of the cone-shaped extrema of the ligaments attached to dripping droplets in the final microseconds before pinchoff. The angle is shown to steadily approach the value of 17.9 $\pm 0.2^\circ$, independent of the initial flow conditions or the type of breakup. The filament thins and necks following a $\tau^{2/3}$ law in terms of the time remaining until pinchoff, regardless of the initial conditions. The observed behaviour confirms theoretical predictions.

PACS numbers: 47.55.df, 47.55.db and 47.80.Jk

Drop formation by jet breakup and pinchoff is a process involved in almost any scenario where a liquid is delivered by jetting and fluid surfaces are broken. Industrial examples of these events occur in inkjet printing, spray deposition and painting, and liquid pipetting, [1]. In addition, there are numerous biological organisms in which droplets are formed through various natural mechanisms [2, 3]. In all these cases, an initially continuous jet is eventually broken up into drops by surface tension forces. Studies of pinchoff and breakup of liquids are not theoretically simple due to finite time singularities and the disparity between dimensional and time scales found in the Navier-Stokes equation describing the dynamics [4, 5]. Experiments in this area are challenging, as they are required to resolve features at very small scales and record events at high speed for long periods of time, in order to capture the fluid behavior during the different time scales involved in breakup [4]. Regardless of these complications, important advances have been achieved in the study of drop formation and breakup. Theoretical and experimental models for Newtonian liquids have confirmed that the Ohnesorge number Oh determines whether a filament condenses into a droplet or breaks up into satellite droplets, where $\mathrm{Oh} = \mu/\sqrt{\rho R_0 \sigma}$, R_0 is the initial radius of the filament, μ is the viscosity, ρ is the density, and σ is the surface tension of the liquid [6–8]. Previous research has demonstrated that the length scale of the pinchoff region of thinning viscous fluids obeys $a \sim \tau \mathrm{Oh}$ scaling, where τ is the time remaining until breakup [4, 5]. Using numerical methods, it has been found that: i) in the pinchoff of inviscid fluids under the action of surface tension, the thinning (neck contraction) follows a scaling law $\sim \tau^{2/3}$, ii) the fluid surface of the droplet overturns before the breakup, and iii) the shape of the breakup region is self-similar and thus independent of initial conditions [4, 9, 10]. By relying on the condition of self-similarity, experimental studies with near-inviscid liquids have demonstrated that this scaling law is followed down to the nanometre and nanosecond scales [11, 12]. Another important conclusion as described in [9] is that, regardless the initial shape of a liquid pendant drop, the breakup angle that the tip of the conical-shaped filament acquires at breakup is 18.1°. Although the theoretically predicted value of the breakup angle has been used to prove the neck-thinning scaling law in some studies [12], an experimental corroboration of the correctness of this value has, however, remained untested. The experimental validation of some aspects of these scaling laws has provided a reliable standard against which to test numerical algorithms that model the formation of droplets by dripping and jetting, [4, 10]. However, given that these simulations usually contain several free parameters, other standards are desirable for further parametric validations, including the breakup angle.

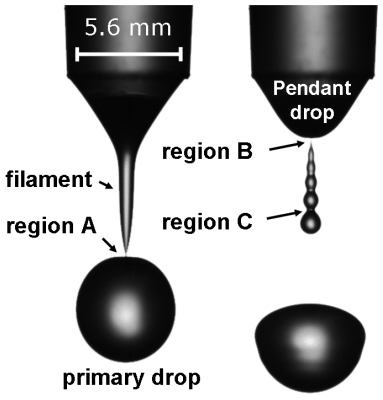

FIG. 1: Breakup regions found in dripping. The breakup at region A forms the primary drop, the breakup in region B detaches the filament from the pendant drop and region C is found at one or several points of breakup within the filament.

In this Letter, the breakup angle and the thinning neck diameter of two near-inviscid liquids are studied under different flow conditions by high speed imaging and image analysis. The results demonstrate that the geometry of pinchoff is self-similar, the necking scaling law is universal, and that the surface breakup angle prior to

breakup is consistent with the previously predicted value of 18.1°.

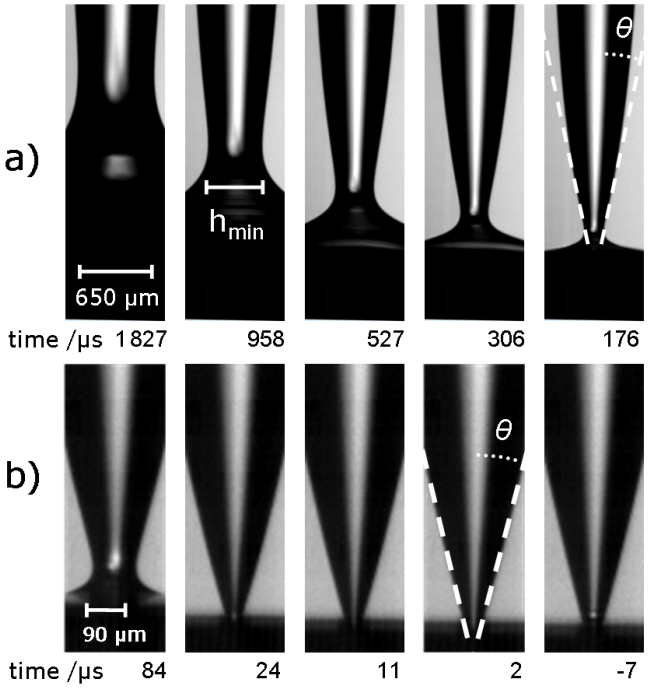

FIG. 2: Imaging of the pinchoff process in region A for a dripping water droplet, the time shown corresponds to the time to breakup. For the conditions observed, the flow is $Q_1^{water} = 0.092$ ml/s. The videos from which these images were extracted were recorded at two camera speeds: in a) the frame rate was 23×10^3 frames/s, and in b) 220×10^3 frames/s. Image analysis was used to extract the angle of the conical filament (θ) from which the droplet is breaking up. Two microseconds prior to breakup (t = 2 μs), $\theta = 16.9 \pm 0.2°$ degrees; the asymptotic analysis shows that at the point of breakup (t=0 μs) $\theta = 17.9 \pm 0.2°$.

For a liquid dripping from a tube at low Oh, breakup can occur at various locations. These are identified as A, B and C in Figure 1. In region A, front-pinching produces the first point of breakup leading to the formation of a main droplet and a filament. In region B, further pinchoff detaches the ligament of liquid from the remaining fluid in the nozzle, forming the so-called satellite filament. In region C, this filament undergoes further breakups forming secondary satellite droplets. In our experiments we acquired high (temporal and spatial) resolution images of these different regions by high speed imaging in a shadowgraph configuration for different flows rates. Image analysis was applied to obtain the breakup angle and the minimum neck diameter. Examples of images for front-pinching (region A) are shown in Figure 2 and examples of the breakup within the filament(region C) are presented in Fig. 3.

The shadowgraph scheme consisted of a 150 W fibre optics lamp (MFO-90, Microtec), an optical diffuser (1" circular engineered microlens array, RPC Photonics) and a high speed camera (Phantom V310, Vision Research)

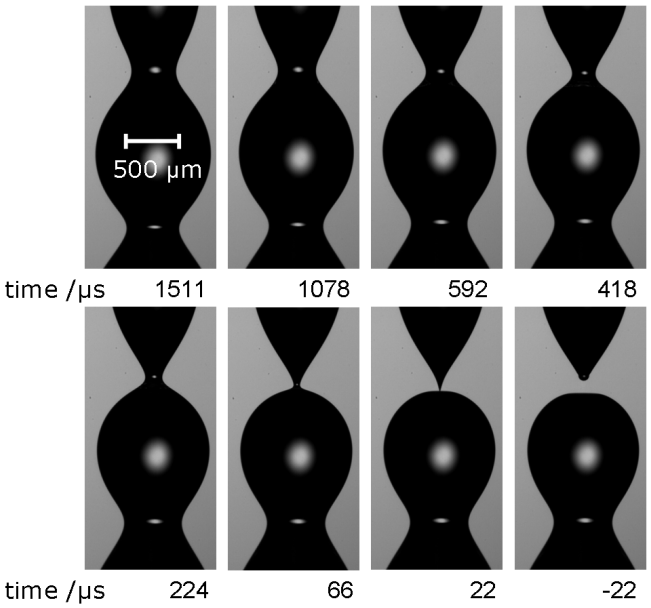

FIG. 3: Imaging of the pinchoff process in region C (filament breakup). The frame rate used in this experiment was 23×10^3 frames/s. For the condition observed, the flow is $Q_4^{water} = 0.750$ ml/s. The asymptotic analysis shows that at the point of breakup (t=0 μs) $\theta = 19.2 \pm 0.9°$.

coupled to a microscope lens (12× ultra zoom, Navitar). Although this optical system is known to produce pincushion distortion at the edges of large CCD sensors [13], the effect is negligible here as only a small central fraction of the sensor is used. This distortion was tested by the imaging of a precision square grid (microscope graticule) at the appropriate frame speeds. The lens-camera configuration was set to a fixed resolution of 193 ± 1 pixels/mm. During the experiments two frame rates were used: 220,000 fps with an exposure time of 1.93 μs and a field of view of 128 × 64 pixels^2, and 23,000 fps with an exposure time of 2.02 μs and a field of view of 512 × 256 pixels^2. Given the finite frame speed and exposure times of the imaging system, the true time of breakup (t) could be determined only to a precision of one half of the interframe time (2.3 μs or 21.7 μs respectively). In these experiments, the exact breakup time is located between those consecutive images showing a connected surface and the evidence of breakup (usually highlighted by the appearance of the bulbous-end formed during the contraction of the filament as seen in the last image of Fig. 2).

Dripping was produced by pumping the liquid from a reservoir to a 12 mm long conical Polymethylpentene plastic nozzle with a measured inlet angle of 4.5° and outlet diameter of 5.6 mm. A sealed and partly-filled liquid container was placed between the pump (Premotec BL58) and the nozzle in order to damp out any irregularity in the pressure and to remove any air bubbles from the liquid; a similar system has been previously used to produce continuous jets [14]. The falling droplets dripped

into the reservoir and the liquid was recirculated by the pump. The working fluids consisted of tri-distilled water and 99.9% ethanol and the experiments were carried out at 21^o C. Fluid density, viscosity and surface tension were measured with an Anton Paar DMA 35N density meter, a Hidramotion 700 Viscolite series viscometer and a SITA bubble pressure t-15 tensiometer (at a bubble lifetime of 500 ms) respectively.

Four different flow rates Q were studied for water and one flow rate for ethanol, as listed in Table 1. The flow rates for experiments with water were chosen to limit the Ohnesorge (Oh) and Weber (We) numbers to that of simple dripping [15] (where We= ρ Q^2/($\pi^2\sigma R^2$), and R is the nozzle radius). Smaller flow rates were limited by the particular characteristics of the fluid pump and the configuration used in this work. Breakup within the filament (region C) was observed only for water at the two highest flows (Q_3^{water} and Q_4^{water}). For lower flow rates the filament did not break up but contracted into a single satellite droplet or recombined with the pendant droplet producing no satellites.

	Q / m^3/s	We	Oh
Q_1^{water}:	9.2 $\times 10^{-8}$	5.4$\times 10^{-4}$	2.2 $\times 10^{-3}$
Q_2^{water}:	2.5 $\times 10^{-7}$	4.0$\times 10^{-3}$	2.2 $\times 10^{-3}$
Q_3^{water}:	5.0 $\times 10^{-7}$	1.6$\times 10^{-2}$	2.2 $\times 10^{-3}$
Q_4^{water}:	7.5 $\times 10^{-7}$	3.9$\times 10^{-2}$	2.2 $\times 10^{-3}$
$Q_1^{ethanol}$:	2.3 $\times 10^{-7}$	8.6$\times 10^{-3}$	7.7 $\times 10^{-3}$

TABLE I: Experimental conditions.

The boundary of inviscid liquid surfaces collapsing just before the pinchoff has been described to be similar to that of a double cone [9], or to the region near the stalk of an apple [11], or of a cone piercing a plate [12]. This geometrical shape is obtained by the overturning of the liquid surface prior to breakup. This overturning is not visible in Figs. 2 and 3 as these images are taken perpendicularly to the direction of jetting, and the pinchoff region is therefore obscured by the fluid between it and the camera. This effect limits the observation of the necking process and the measurement of h$_{min}$, [4]. Images were analyzed to determine the minimum visible neck and the small angle of pinchoff (α_{small}) at various times. This process was carried out in Matlab by superimposing straight lines on to the fluid boundaries on the small angle side from h = h$_{min}$ to 4h$_{min}$. The small pinchoff angle is therefore half the angle between these linear fits. Although the surface overturning prevented the direct measurement of the angle at the point of minimum neck width, the angle was measured on the surface directly before the overturning point. Shadowgraphy was particularly useful for this analysis as it produces images with very high contrast which consequently reduces the experimental error. Results are shown in Figures 4 and 5.

The effects of gravity are considered unimportant for flows on shorter scales than the gravitational capillary

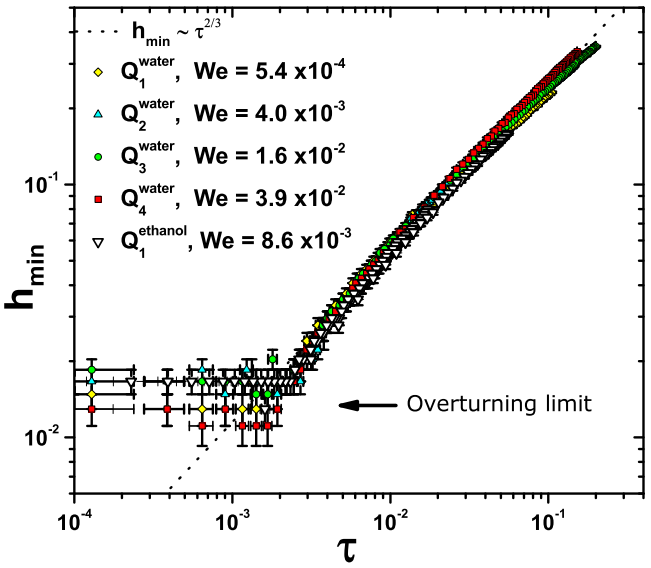

FIG. 4: (Colour online) Experimental measurements of the minimum neck diameter (h$_{min}$) in terms of the dimensionless time (τ) to breakup for different fluids and different flows. Regardless of the condition of flow, within simple dripping the thinning follows a self-similar behavior. The broken line represents the potential flow scaling law. The measurement of h$_{min}$ is limited by the overturning of the droplet surface.

length $l_G = \sqrt{2\sigma/\rho g}$ and are negligible near the breakup, [16]. Under these experimental conditions, $l_G^{water} = 3.8$ mm and $l_G^{ethanol} = 2.4$ mm. Given that the field of view of our imagining system only permits the observation of smaller flows than these values, the effects of gravity on the experimental results presented in this Letter can be ignored. The inertia of the surrounding air becomes important only when the neck thinning approaches the limit $\sim h_{min}(\mu_{air}\mathrm{Oh}^2/\mu)$, where μ_{air} is the air viscosity, [17]. In these experiments, $h_{min}^{water} = 0.3$ nm and $h_{min}^{ethanol} = 1.7$ nm, both beyond the optical resolution of the imaging setup. Aerodynamic and inertial effects influence the breakup process when the gas Weber number We$_g > 0.2$, where We$_g = (\rho_g/\rho)$We and ρ_g is the density of air, [18]. In this work, We$_g^{water}$ ranges from 6.5×10^{-7} to 4.5×10^{-5} and We$_g^{ethanol} = 1.3 \times 10^{-5}$. Consequently these effects can also be considered negligible.

The first set of results, shown in Fig. 4 have been put in dimensionless form by using the nozzle radius and the capillary time $t_c = \sqrt{\rho R^3/\sigma}$, so that $\tau = t/t_c$. Figure 4 shows that the neck thinning near the breakup is consistent with the scaling law h$_{min} \sim \tau^{2/3}$ regardless of the flow initial conditions or the liquid properties. The observed overturning limit is also consistent with previous experimental and numerical results obtained for a different (single) flow, [4].

Self-similarity is a geometrical property that in liquids can be assessed by analyzing surface shapes. Figure 5 shows the evolution of the small angle in terms of the time to breakup for different flow conditions, different regions

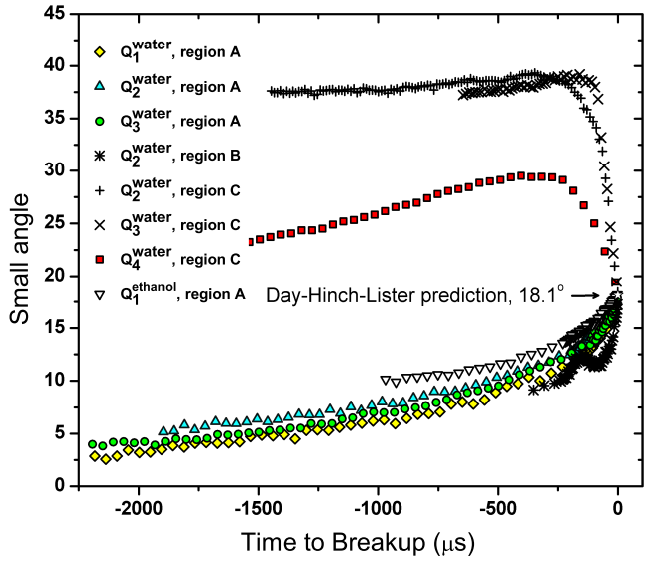

FIG. 5: (Colour online) Small pinchoff angle for different flow conditions, breakup regions and fluids. The mean of the convergent angle value for all the cases is $\alpha_{small} = 17.94 \pm 0.20°$.

of breakup, and different fluids. For the experiments in Region A the small angle slowly evolves from very small angles (as the filament is initially almost cylindrical) with a rapid increase during the final few microseconds before the breakup. In region B, the satellite filament undergoes further deformation and multiple breakups that generate secondary satellite droplets. This interesting dynamics shows an alternate route to breakup as there is no pre-existing filament from where a 'main' drop can pinch off, but the process starts with two (or more) bulbous regions of fluid, separated by a contracting neck. The angle therefore, affected greatly by the rapid neck contraction, follows a different path: it evolves from large values to a maximum for several hundreds of microseconds and then decays rapidly, reaching the much smaller angle during the final tens of microseconds prior breakup. These rather different dynamics permits the study of breakup from two different approaching directions (from angles >18.1° and <18.1°). Region C presents somewhat different dynamics, as it is affected by the primary breakup (the detachment of the main droplet). As soon as the main droplet breaks from the filament, the latter rapidly contracts and excites capillary waves that travel all the way up to the contracting neck where the filament detaches from the fluid in the nozzle (breakup region C). This generates an oscillatory effect in the evolution of the small angle. This is clearly observed in the plotted data of Fig. 5. It is also important to note that during the final moments before breakup, however, such oscillation is no longer evident and the small angle follows a similar behaviour to that of Region A.

As can be observed in Fig. 5 all the experimental data asymptotically approach a common angle at breakup. Following [9], the asymptotic value was calculated by plotting the small angle as a function of $\tau^{1/2}$ giving an adequately straight line for the last 80 μs before breakup; the final cone angle was deduced by extrapolation from these linear fits. In all the cases explored in this work the extrapolated angle was never outside the confidence interval of $2\sigma_s$ from the theoretical value of 18.1° (where σ_s is the experimental error). It is remarkable that regardless of the flow, which effectively controls the the initial shape of the fluid, the final angle of breakup approaches the same asymptotic value, *i.e.* the breakup is self-similar. In summary, the results presented in this Letter show that the geometry of the breakup of near-inviscid fluids is self-similar in the domain of simple dripping. It has also been shown that, independent of initial conditions and fluid characteristics, the necking of the liquid liquid scales with $\tau^{2/3}$ and asymptotically approaches a unique angle of 17.9 ± 0.2 degrees.

This project was supported by the UK Engineering and Physical Sciences Research Council through the GlassJet and I4T projects (Grants EP/G029458/1 and EP/H018913/1).

[1] O.A. Basaran, *AIChE Journal* **48** 1842 (2002).
[2] T. Schlegel, C.J. Schmid and S. Schuster, *Current Biology* **16**, R836-R837 (2006).
[3] T. Eisner and D.J. Aneshansley, *Proc Natl Acad Sci USA* **96**, 69705-9706 (1999).
[4] A.U. Chen, P.K. Notz and O.A. Basaran, *Phys. Rev. Lett.* **88** 174501 (2002).
[5] J. Eggers, *Phys. Rev. Lett.* **71** 3458 (1993).
[6] R.M.S.M. Schulkes, *J. Fluid. Mech.* **309** 277 (1996).
[7] P.K. Notz and O.A. Basaran, *J. Fluid Mech.* **512** 223 (2004).
[8] A.A. Castrejón-Pita, J.R. Castrejón-Pita and I. M. Hutchings, *Phys. Rev. Lett.* **108** 074506 (2012).
[9] R.F. Day, E.J. Hinch and J.R. Lister, *Phys. Rev. Lett.* **80** 704 (1998).
[10] J.R. Castrejón-Pita, N.F. Morrison, O.G. Harlen, G.D. Martin and I. M. Hutchings, *Phys. Rev. E* **83** 036306 (2011).
[11] J.C. Burton, J.E. Rutledge and P. Taborek, *Phys. Rev. Lett.* **92** 244505 (2004).
[12] J.C. Burton, J.E. Rutledge and P. Taborek, *Phys. Rev. E.* **75** 036311 (2007).
[13] J.R. Castrejón-Pita, G.D. Martin and I.M. Hutchings, *J. Imaging Sci. Technol.* **55** 040305 (2011).
[14] J.R. Castrejón-Pita, N.F. Morrison, O.G. Harlen, G.D. Martin and I. M. Hutchings, *Phys. Rev. E* **83** 016301 (2011).
[15] B. Ambravaneswaran, H.J. Subramani, S.D. Phillips and O.A. Basaran, *Phys. Rev. Lett.* **93** 0134501 (2004).
[16] A.U. Chen and O.A. Basaran, *Phys. Fluids* **14** L1 (2002).
[17] J.R. Lister and H.A. Stone, *Phys. Fluids* **10** 2758 (1998).
[18] W. Hoeve *et al.*, *Phys. Fluids* **22** 122003 (2010).